Strange quark distributions in the ABMP16 fit and beyond

S.Alekhin (*Univ. of Hamburg & IHEP Protvino)*

sa, Blümlein, Moch, Plačakytė PRD 96, 014011 (2017)
sa, Blümlein, Moch PLB 777, 134 (2018)

LHC Physics Discussion, DESY, 25 Mar 2019

PDF fit framework

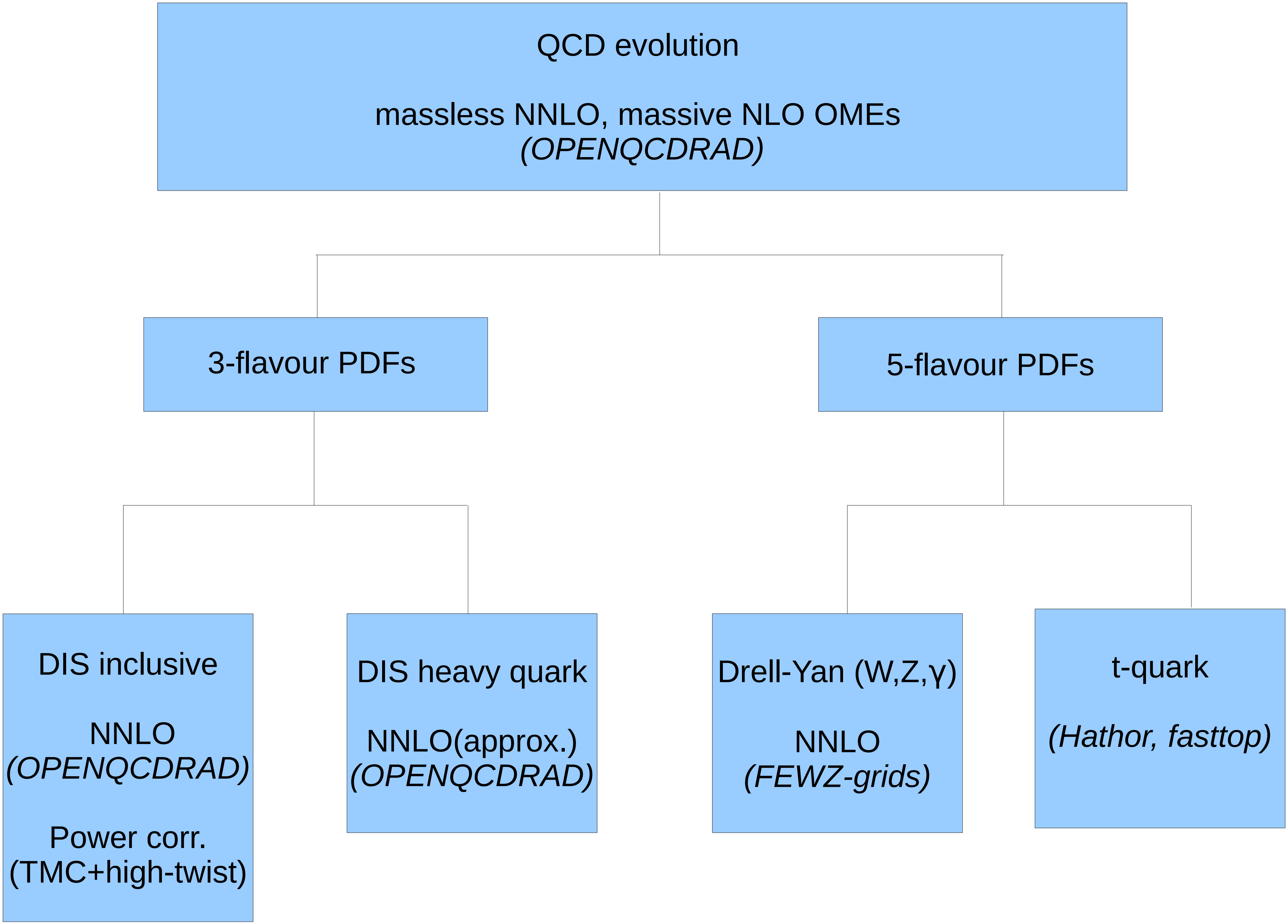

Data used and fit quality

Experiment	Process	Reference	NDP	χ^2
	DIS			
HERA I + II	$e^\pm p \to e^\pm X$	[4]	1168	1510
	$e^\pm p \to \overset{(-)}{\nu} X$			
BCDMS	$\mu^+ p \to \mu^+ X$	[61]	351	411
NMC	$\mu^+ p \to \mu^+ X$	[60]	245	343
SLAC-49a	$e^- p \to e^- X$	[54,62]	38	59
SLAC-49b	$e^- p \to e^- X$	[54,62]	154	171
SLAC-87	$e^- p \to e^- X$	[54,62]	109	103
SLAC-89b	$e^- p \to e^- X$	[56,62]	90	79
	DIS heavy-quark production			
HERA I + II	$e^\pm p \to e^\pm cX$	[63]	52	62
H1	$e^\pm p \to e^\pm bX$	[15]	12	5
ZEUS	$e^\pm p \to e^\pm bX$	[16]	17	16
CCFR	$\overset{(-)}{\nu} N \to \mu^\pm cX$	[64]	89	62
CHORUS	$\nu N \to \mu^+ cX$	[18]	6	7.6
NOMAD	$\nu N \to \mu^+ cX$	[17]	48	59
NuTeV	$\overset{(-)}{\nu} N \to \mu^\pm cX$	[64]	89	49
	DY			
FNAL-605	$pCu \to \mu^+\mu^- X$	[68]	119	165
FNAL-866	$pp \to \mu^+\mu^- X$	[69]	39	53
	$pD \to \mu^+\mu^- X$			
	Top-quark production			
ATLAS, CMS	$pp \to tqX$	[27–32]	10	2.3
CDF&DØ	$\bar{p}p \to tbX$	[53]	2	1.1
	$\bar{p}p \to tqX$			
ATLAS, CMS	$pp \to t\bar{t}X$	[33–52]	23	13
CDF&DØ	$\bar{p}p \to t\bar{t}X$	[53]	1	0.2

Direct constraint on strangeness (CCFR, CHORUS, NOMAD, NuTeV)

Collider DY in the next slide (indirect constraint on strangeness)

DY data in the ABMP16 fit

Experiment	ATLAS		CMS		DØ		LHCb		
$\sqrt{s}$ (TeV)	7	13	7	8	1.96		7	8	
Final states	$W^+ \to l^+\nu$ $W^- \to l^-\nu$ $Z \to l^+l^-$	$W^+ \to l^+\nu$ $W^- \to l^-\nu$ $Z \to l^+l^-$	$W^+ \to \mu^+\nu$ $W^- \to \mu^-\nu$ (asym)	$W^+ \to \mu^+\nu$ $W^- \to \mu^-\nu$	$W^+ \to \mu^+\nu$ $W^- \to \mu^-\nu$ (asym)	$W^+ \to e^+\nu$ $W^- \to e^-\nu$ (asym)	$W^+ \to \mu^+\nu$ $W^- \to \mu^-\nu$ $Z \to \mu^+\mu^-$	$Z \to e^+e^-$	$W^+ \to \mu^+\nu$ $W^- \to \mu^-\nu$ $Z \to \mu^+\mu^-$
Cut on the lepton P_T	$P_T^l > 20$ GeV	$P_T^e > 25$ GeV	$P_T^\mu > 25$ GeV	$P_T^\mu > 25$ GeV	$P_T^\mu > 25$ GeV	$P_T^e > 25$ GeV	$P_T^\mu > 20$ GeV	$P_T^e > 20$ GeV	$P_T^\mu > 20$ GeV
Luminosity (1/fb)	0.035	0.081	4.7	18.8	7.3	9.7	1	2	2.9
NDP	30	6	11	22	10	13	31(33) [a]	17	32(34)
ABMP16	31.0	9.2	22.4	16.5	17.6	19.0	45.1(54.4)	21.7	40.0(59.2)
CJ15	–	–	–	–	20	29	–	–	–
CT14	42	–	– [b]	–	–	34.7	–	–	–
HERAFitter	–	–	–	–	13	19	–	–	–
MMHT16	39 [c]	–	–	21	21 [c]	26	(43)	29	(59)
NNPDF3.1	29	–	19	–	16	35	(59)	19	(47)

[a] The values of NDP and χ^2 correspond to the unfiltered samples.
[b] For the statistically less significant data with the cut of $P_T^\mu > 35$ GeV the value of $\chi^2 = 12.1$ was obtained.
[c] The value obtained in MMHT14 fit.

Experiment	NDP	χ^2 after the data sets excuded				
		–	ATLAS	CMS	DØ	LHCb
ATLAS	36	37.7	–	37.0	38.3	39.6
CMS	33	26.6	25.6	–	26.0	23.5
DØ	23	48.5	48.1	47.7	–	**44.2**
LHCb	80	98.2	100.2	97.4	**78.8**	–

- Good overall agreement in NNLO with some tension between D0 and LHCb data

Strange sea from the νN DIS

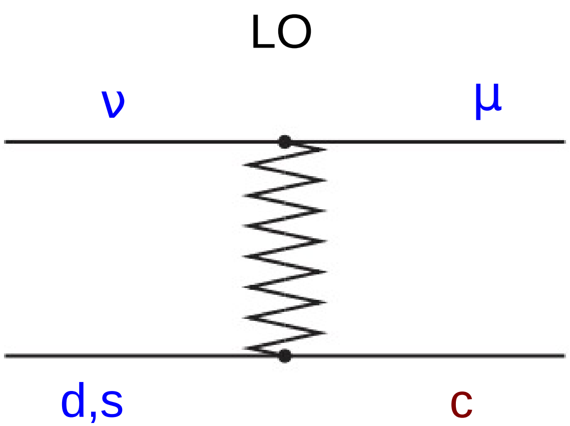

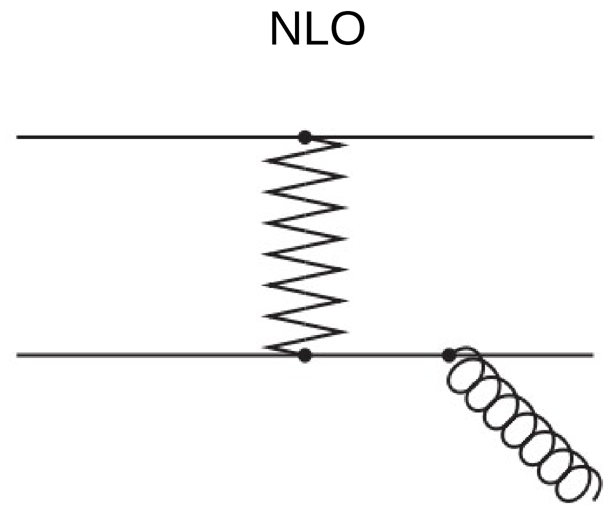

Two decay modes of c-quark are used: hadronic (emulsion experiments) and semi-leptonic (electronic experiments)

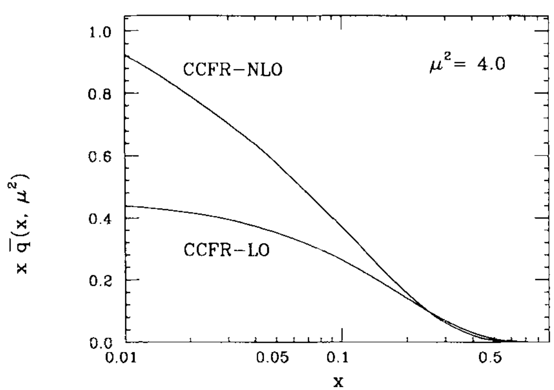

Fig. 3. The quark sea distribution $x\bar{q}(x, \mu^2 = 4.0\,\mathrm{GeV}^2/c^2)$ determined at next-to-leading order and leading order

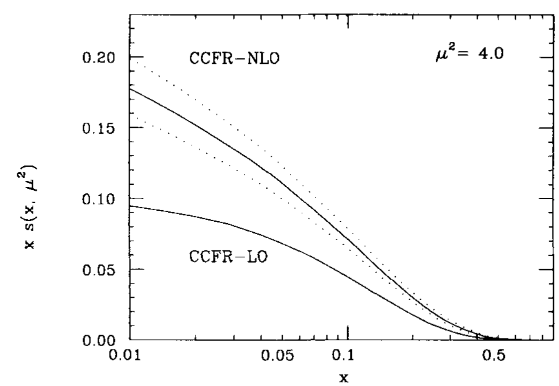

Fig. 4. The strange quark distribution $xs(x, \mu^2 = 4.0\,\mathrm{GeV}^2/c^2)$ determined at next-to-leading order (described in section 4.1) and leading order. The band around the NLO curve indicates the $\pm 1\sigma$ uncertainty in the distribution

CCFR ZPC 65, 189 (1995)

Primary source for the strange sea was for a long time neutrino-induced charm production measured by CCFR/NuTeV at Fermilab preferring a suppression of ~0.5 w.r.t. non-strange sea

NuTeV/CCFR data in the PDF fit framework

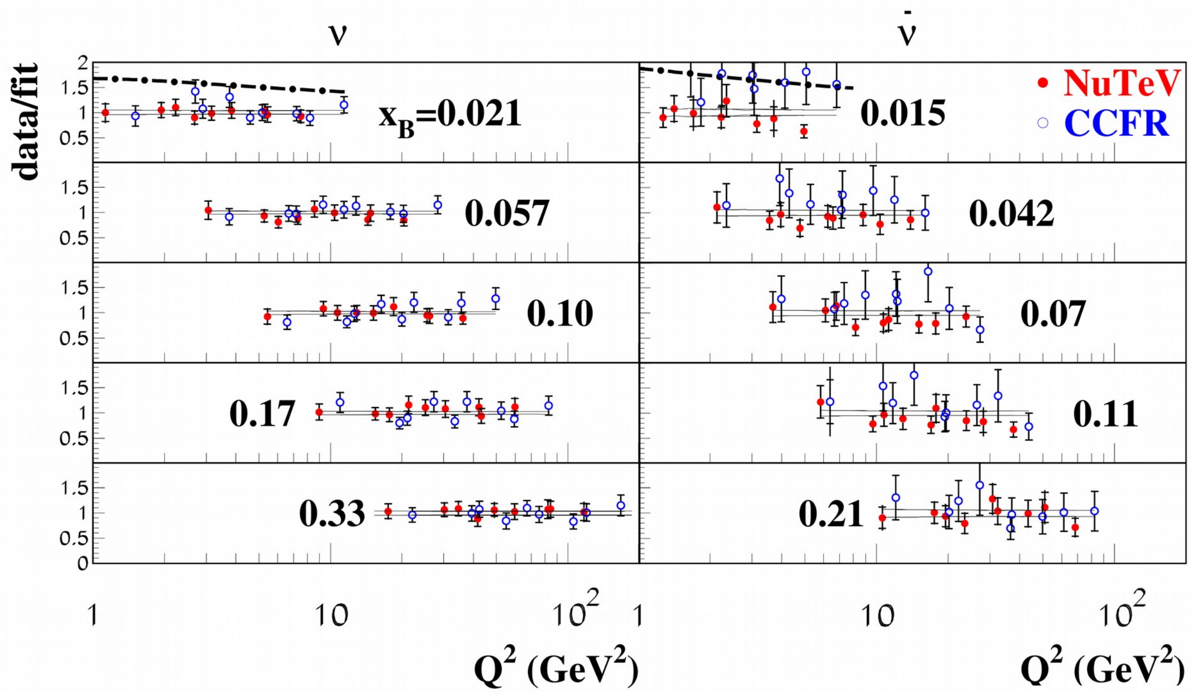

- CCFR and NuTeV are in a good agreement
- Charge asymmetry in the strange sea is consistent with 0 within uncertainties

sa, Kulagin, Petti PLB 675, 433 (2009)

$$\kappa_s(\mu^2) = \frac{\int_0^1 x[s(x,\mu^2)+\bar{s}(x,\mu^2)]dx}{\int_0^1 x[\bar{u}(x,\mu^2)+\bar{d}(x,\mu^2)]dx},$$

Integral suppression factor
K_s(20 GeV^2)=0.62±0.04 is obtained

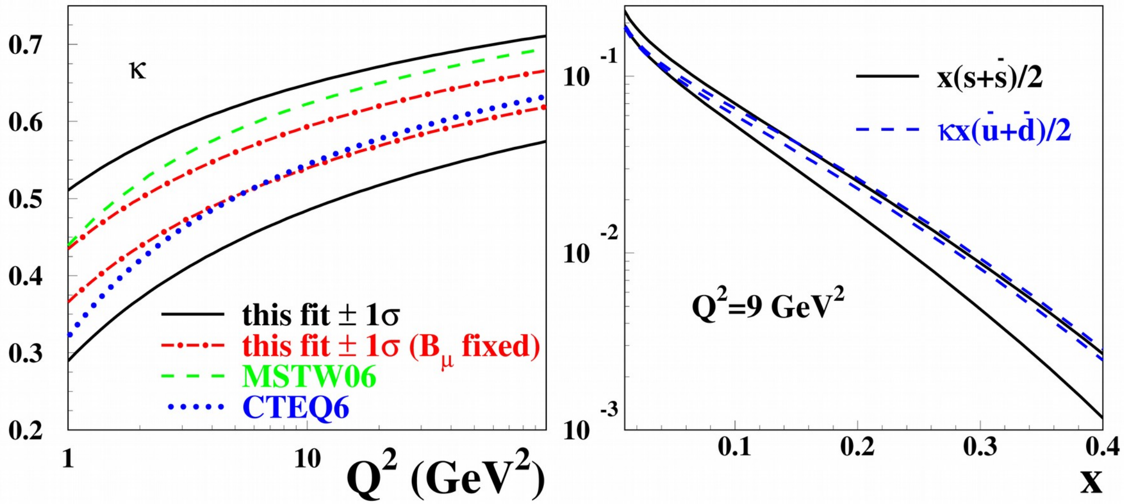

NOMAD charm data

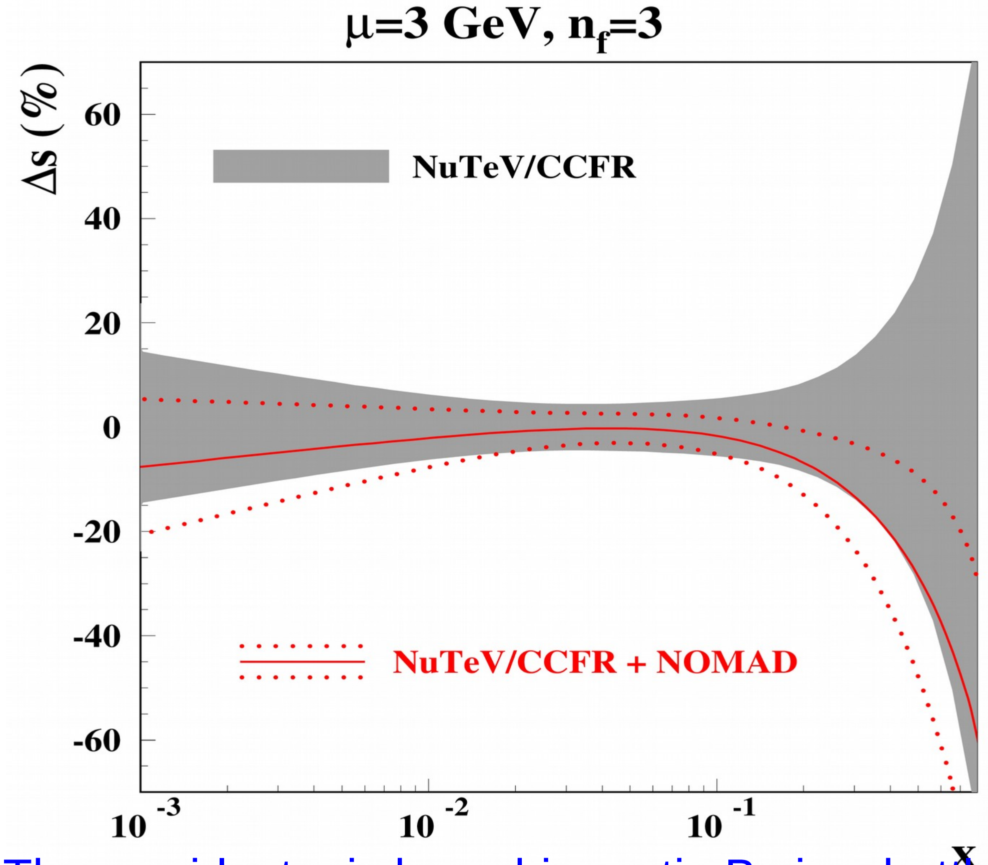

NOMAD NPB 876, 339 (2013)

- The data on ratio 2μ/incl. CC ratio with the 2μ statistics of 15000 events (much bigger than in earlier CCFR and NuTeV samples).
- Systematics, nuclear corrections, etc. cancel in the ratio
- Pull down strange quarks at x>0.1 with a sizable uncertainty reduction

The semi-leptonic branching ratio B_μ is a bottleneck

– weighted average of the charmed-hadron rates

$$B_\mu(E_\nu)=\sum_h r^h(E_\nu)B^h_\mu = a/(1+b/E_\nu)$$

– fitted simultaneously with the PDFs, etc. using the constraint from the emulsion data

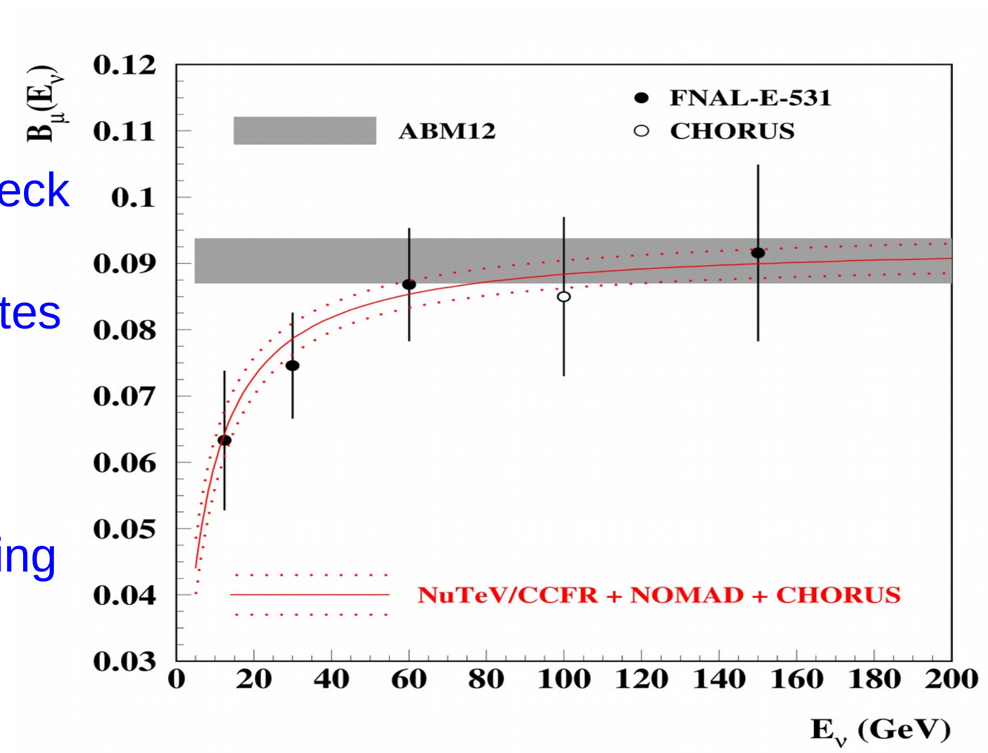

Constraints on strange sea

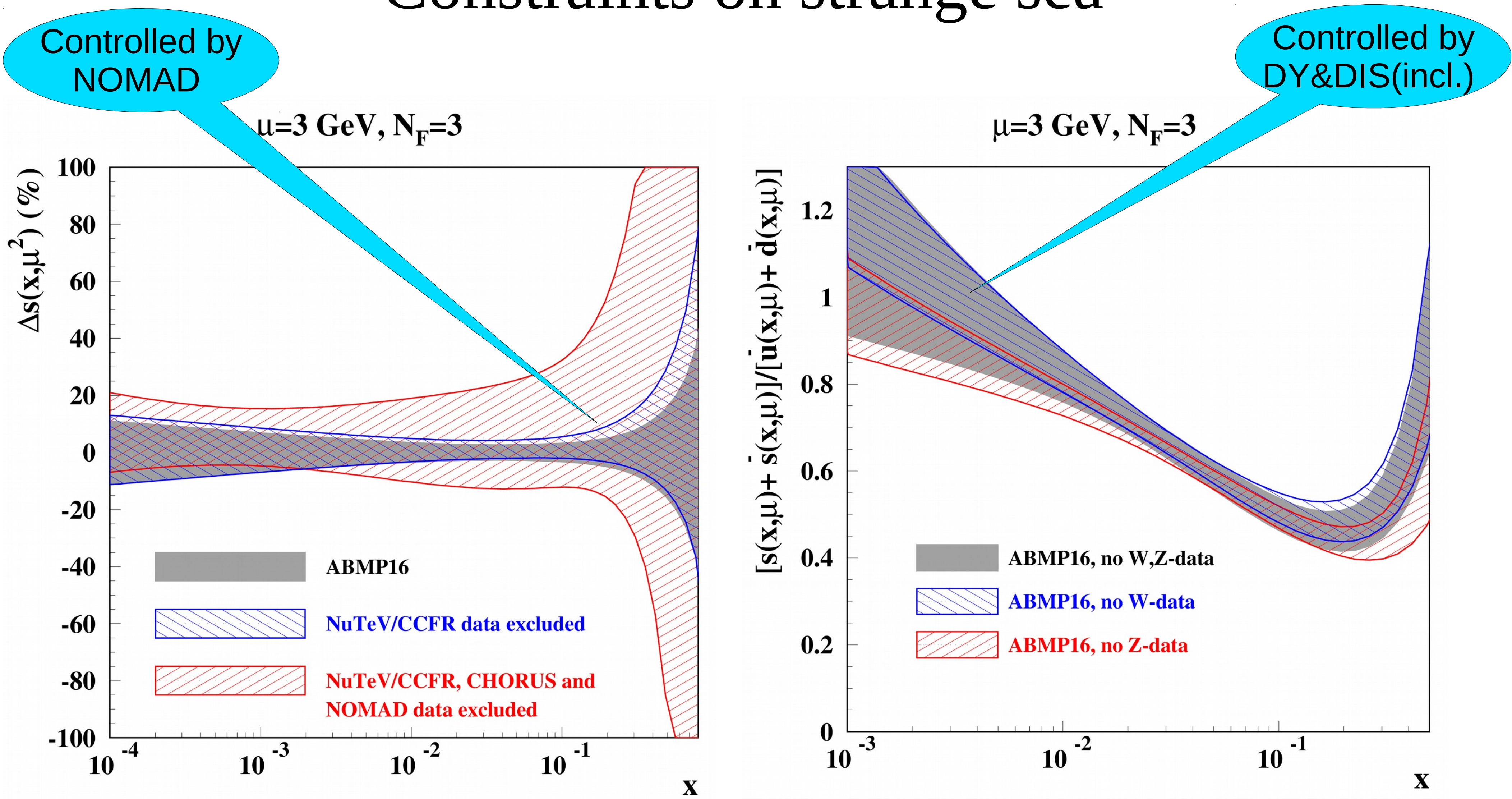

- Uncertainty of ~5% is achieved at x around 0.1
- NuTeV/CCFR data play no essential role → impact of the nuclear corrections is greatly reduced (NOMAD and CHORUS give the ratio CC/incl.)

Nuclear corrections in NOMAD data

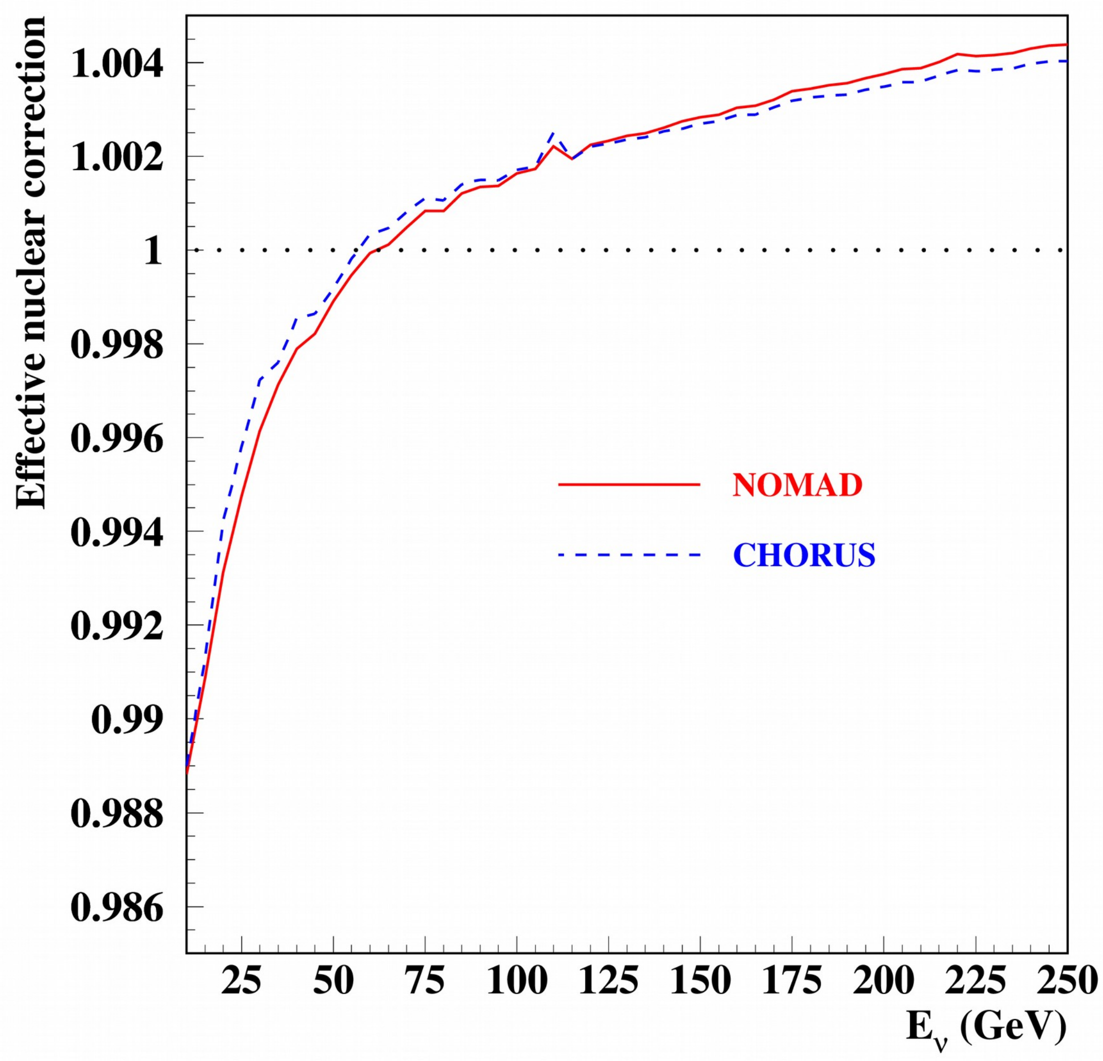

Nuclear corrections cancel in the ratio

ATLAS strange enhancement

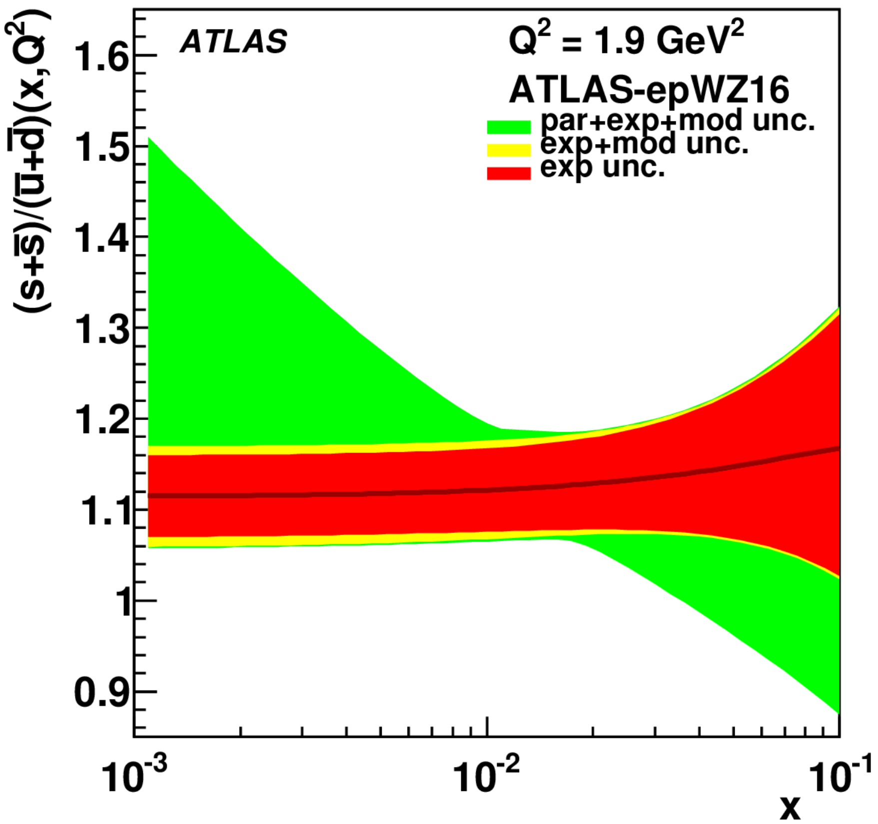

ATLAS arXiv:1612.03016

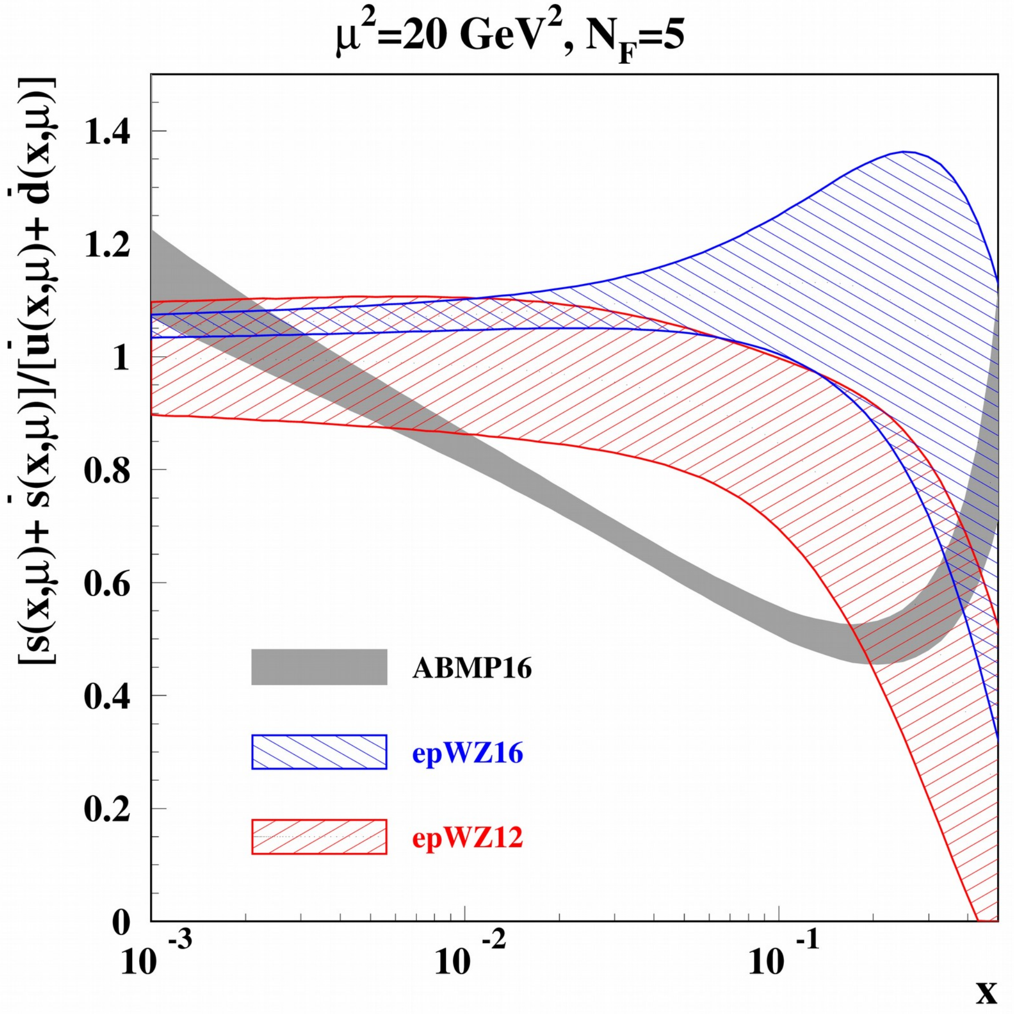

The epWZ16 strange-sea determined from analysis of the combined HERA-ATLAS data is enhanced as compared to other (earlier) determinations

ABM strange sea determination is in particular based on the dimuon neutrino-nucleon DIS production (NuTeV/CCFR and NOMAD) that gives a strange sea suppression ~0.5 at x~0.2

- *Disentangling d- and s- contribution?*
- *Impact of the nuclear corrections?*
- *…..?*

Test-fit data set (epWZ16 and CJ15 studies)

sa, Blümlein, Moch PLB 777, 134 (2018)
sa, Blümlein, Kulagin, Moch, Petti hep-ph/1808.06871

Experiment	Process	NDP
DIS		
HERA I+II	$e^{\pm}p \to e^{\pm}X$ $e^{\pm}p \to \overset{(-)}{\nu} X$	1168
Fixed-target (BCDMS, NMC, SLAC)	$l^{\pm}p \to l^{\pm}X$	1935
DIS heavy-quark production		
HERA I+II	$e^{\pm}p \to e^{\pm}cX$	52
H1, ZEUS	$e^{\pm}p \to e^{\pm}bX$	29
Fixed-target (CCFR, CHORUS, NOMAD, NuTeV)	$\overset{(-)}{\nu} N \to \mu^{\pm}cX$	232
DY		
Fixed-target (FNAL-605, FNAL-866)	$pN \to \mu^{+}\mu^{-}X$	158

The ABMP16 framework with:

– DY data replaced by the deuteron ones ⇒ comparable quark disentangling at moderate and large x

– t-quark data excluded (no relevance for present study)

Test fit (the PDF shape comparison)

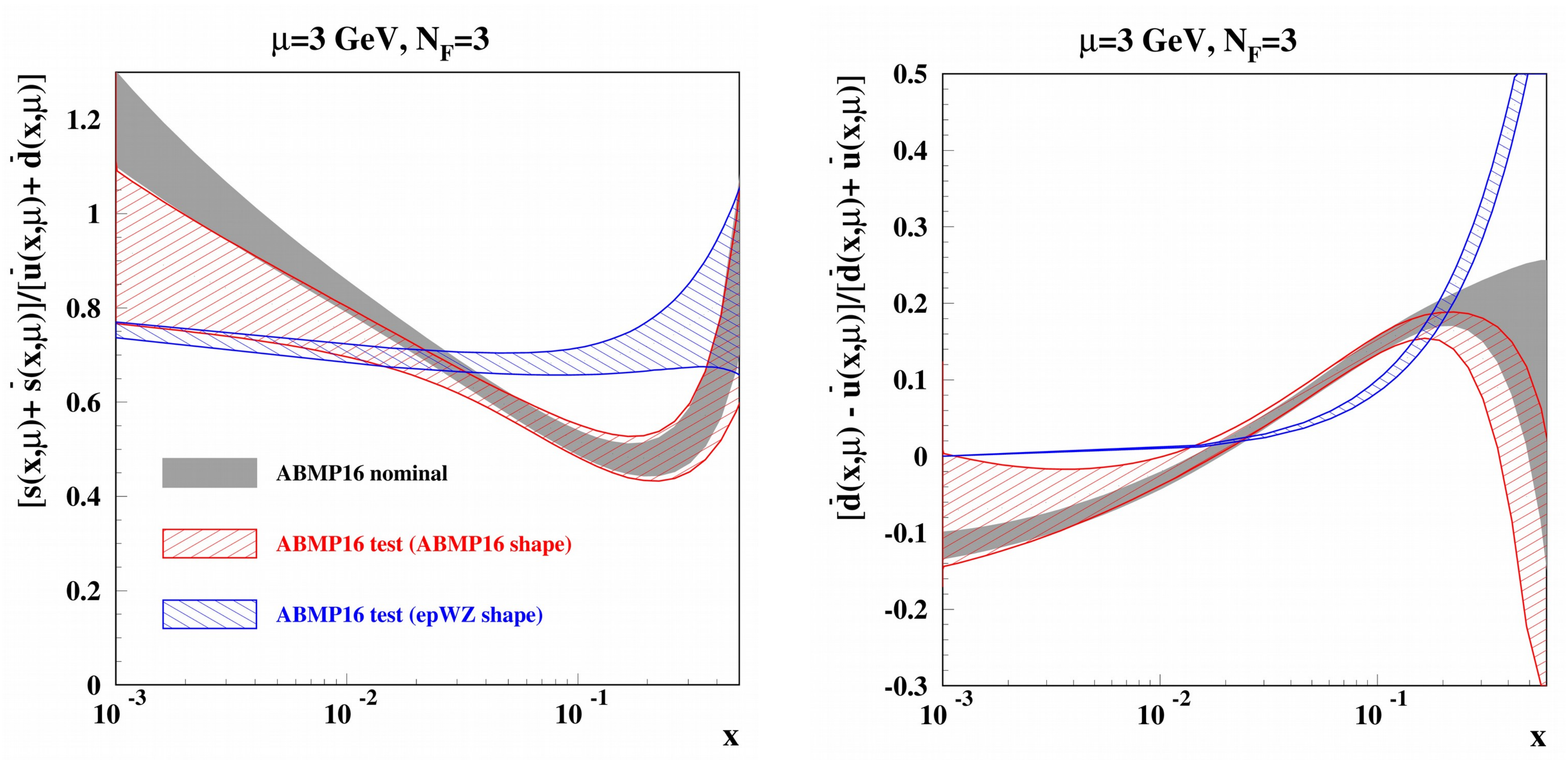

The strange sea is enhanced for the epWZ shape despite the ATLAS data are not used. However, the dimuon data description is not deteriorated: χ^2=167 versus 161 for the ABMP shape ⇒ enhancement is achieved by the price of the d-quark sea suppression

sa, Blümlein, Caminada, Lipka, Lohwasser, Moch, Petti, Plačakytė PRD 91, 094002 (2015)

Checking styles of PDF shape

	ABMP16	CJ15	CT10	CT14	epWZ16	MMHT14
N_{PDF}	28	21	26	26	14	31
μ_0^2 (GeV^2)	9	1.69	1.69	1.69	1.9	1
χ^2	4065	4108	4148	4153	4336	4048
PDF shape	$x^{\alpha}(1-x)^{\beta}$ $\exp[P(x,\ln(x))]$	$x^{\alpha}(1-x)^{\beta}P(x,\sqrt{x})$	$x^{\alpha}(1-x)^{\beta}$ $\exp[P(x,\sqrt{x})]$	$x^{\alpha}(1-x)^{\beta}$ $\exp[P(x,\sqrt{x})]$	$x^{\alpha}(1-x)^{\beta}P(x,\sqrt{x})$	$x^{\alpha}(1-x)^{\beta}P(x,\sqrt{x})$
Constraints		$\bar{u}=\bar{d}$ $(x\rightarrow 0)$	$\alpha_{uv}=\alpha_{dv}$ $\alpha_{\bar{u}}=\alpha_{\bar{d}}=\alpha_s$ $\bar{u}=\bar{d}$ $(x\rightarrow 0)$	$\alpha_{uv}=\alpha_{dv}$ $\beta_{uv}=\beta_{dv}$ $\alpha_{\bar{u}}=\alpha_{\bar{d}}=\alpha_s$	$\alpha_{\bar{u}}=\alpha_{\bar{d}}=\alpha_s$ $\bar{u}=\bar{d}$ $(x\rightarrow 0)$	
$\alpha_s(M_Z)$	0.1153	0.1147	0.1150	0.1160	0.1162	0.1158

- Various PDF-shape modifications provide comparable description with N_{PDF}~30
- Some deterioration, which happens in cases is apparently due to constraints on large(small)-x exponents

E866 data in the test fit

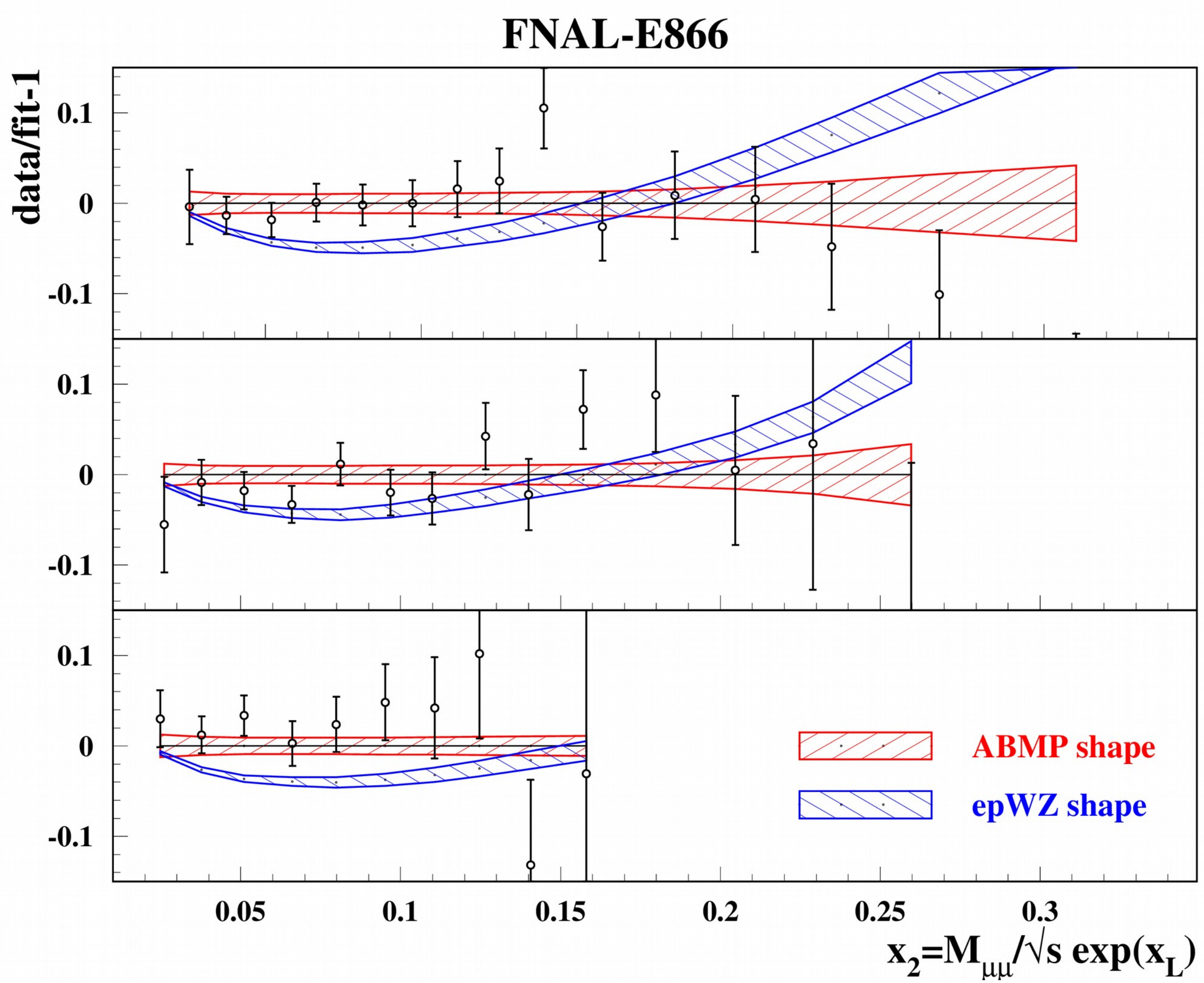

The E866 data on p/d DY cross sections are sensitive to the iso-spin sea asymmetry

The epWZ shape does not allow to accommodate E866 data: χ^2/NDP=96/39 versus 49/39 for the ABMP shape; the errors in epWZ predictions are suppressed at small x, evidently due to over-constrained PDF shape at small x

Consistency of ATLAS and E866 data

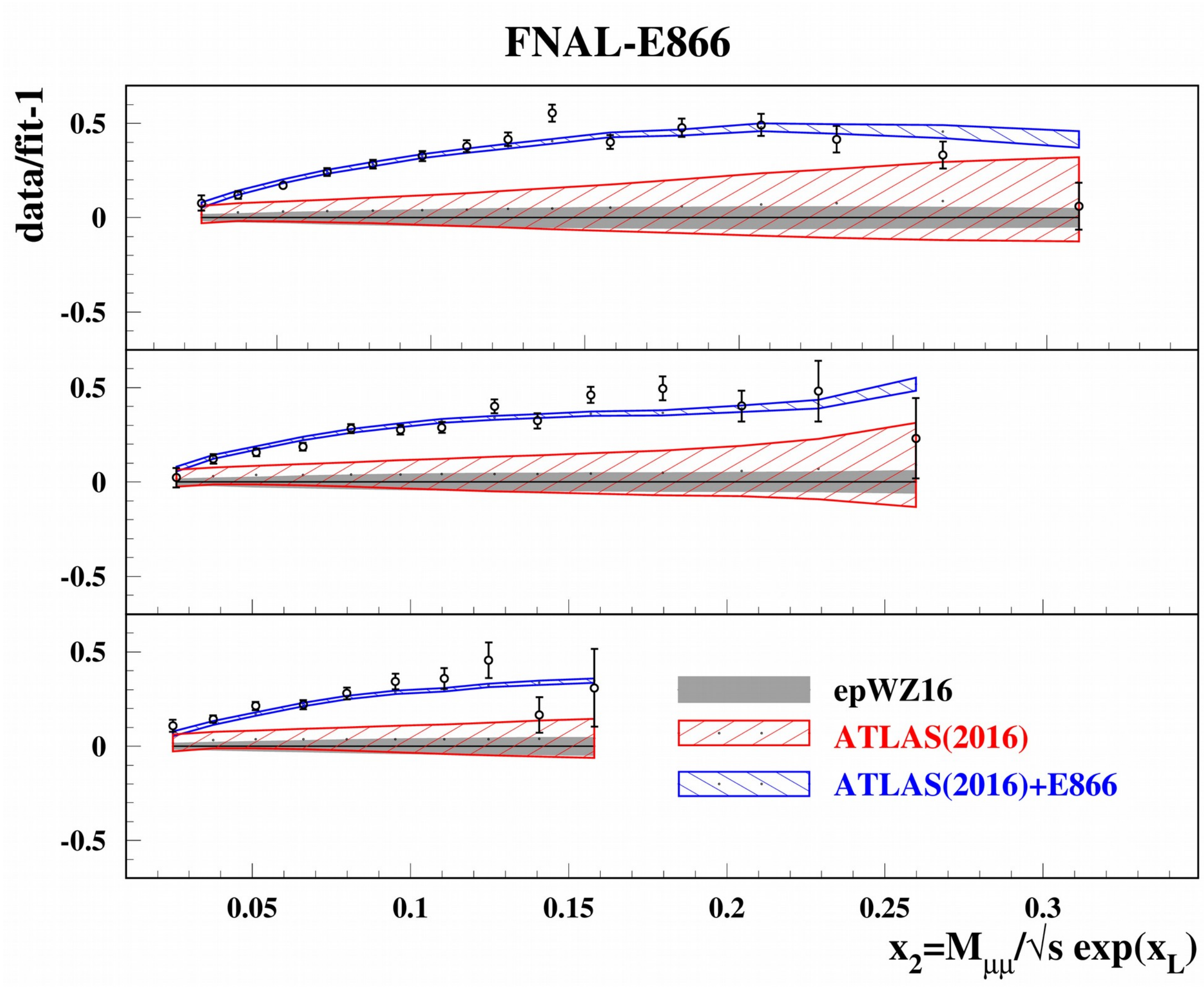

- The uncertainties in epWZ predictions are quite narrow and several σ off the E866 data ⇒ E866 cannot be accommodated into the fit

ATLAS

- The ABMP16 shape gives much wider error band ⇒ E866 data are well accommodated: χ^2/NDP=48/39 and 40/34 for the E866 and ATLAS, respectively

Closure test of the NN31 fit

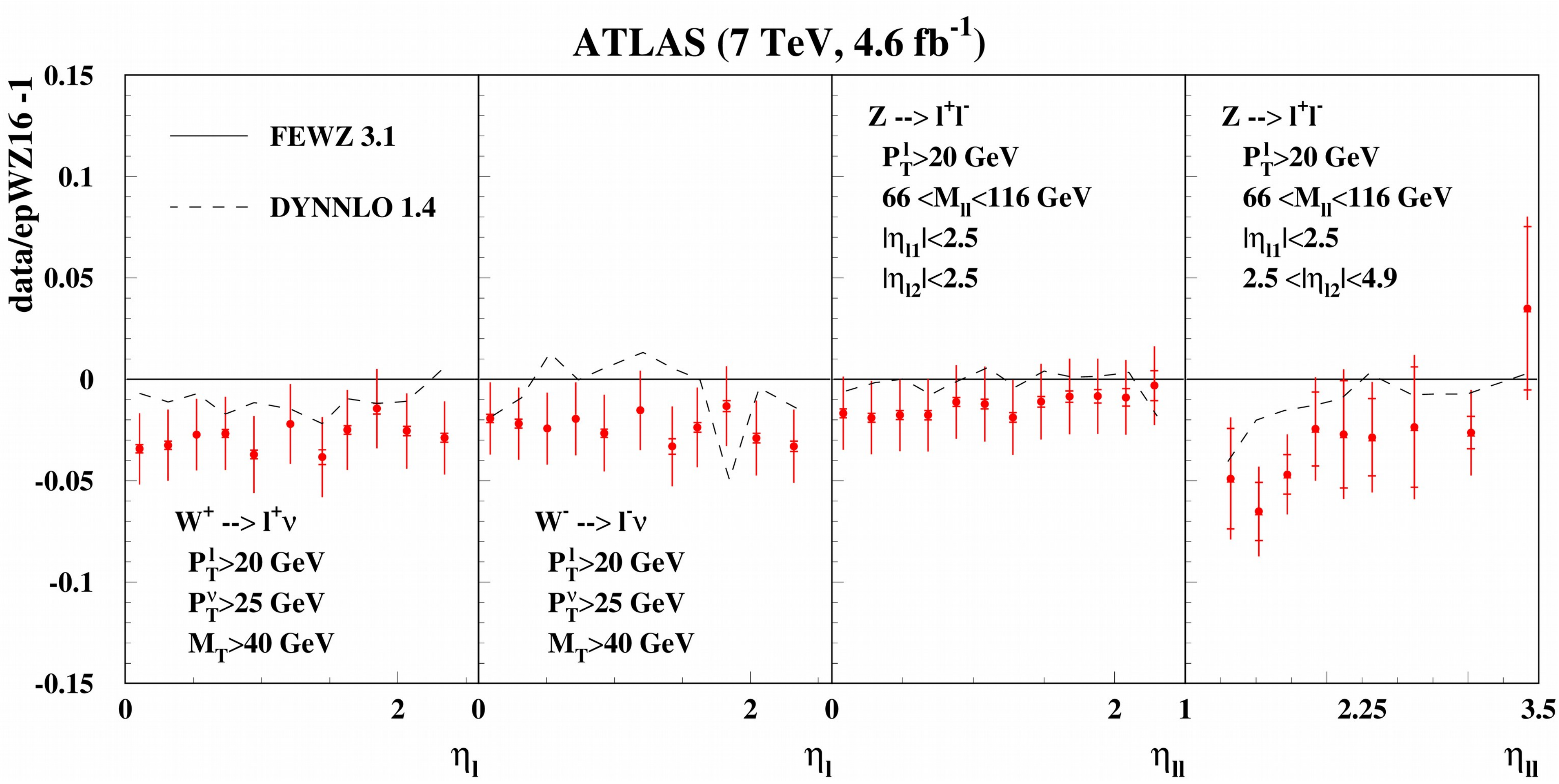

The epWZ16 predictions go systematically above the ATLAS data ⇒ either statistical bias or inaccurate theory predictions (epWZ16 fit uses combination of the NLO calculations with the NNLO K-factors)

Closure test of the NNPDF3.1 fit

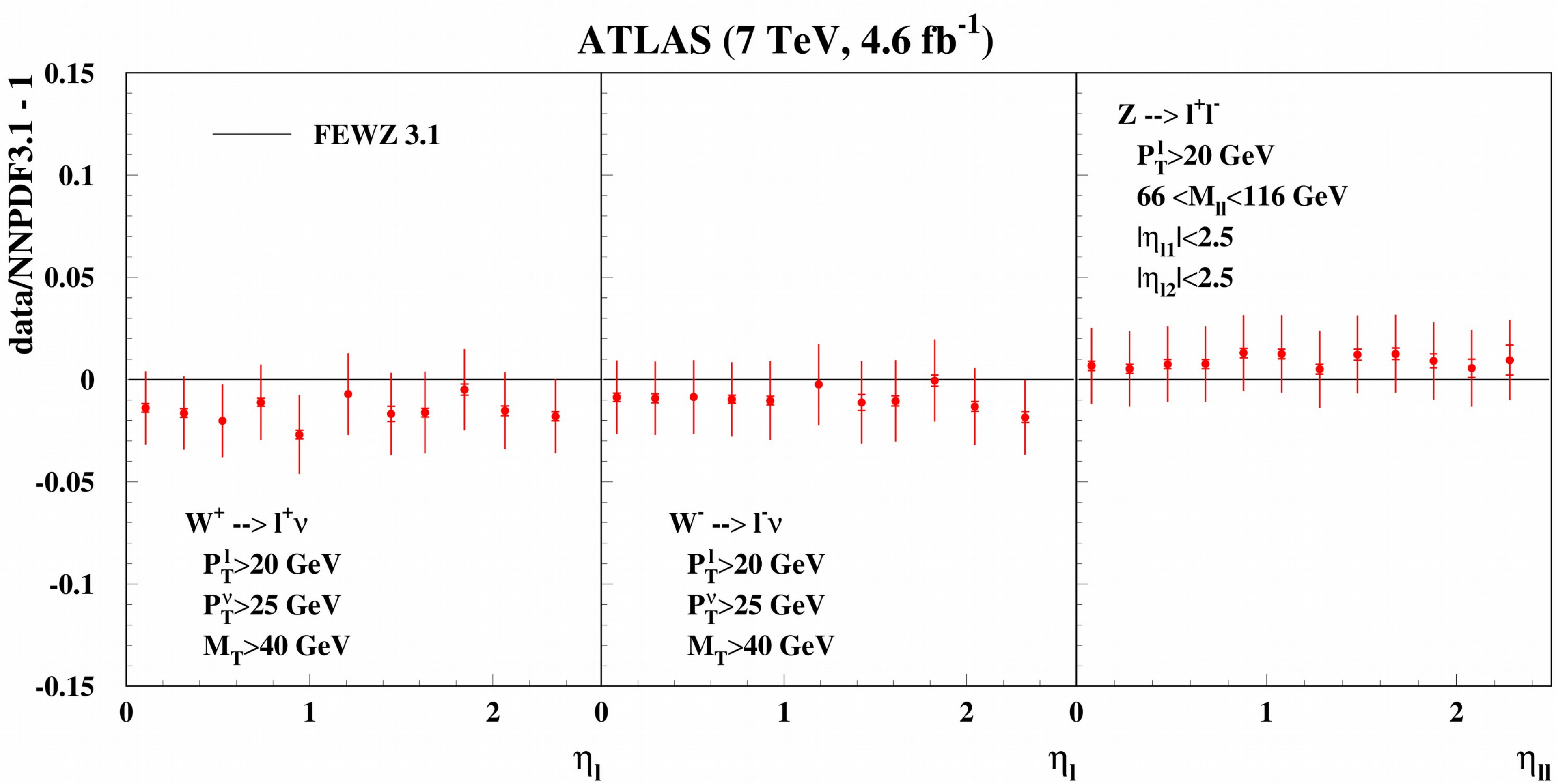

- Different trend for W and Z data ⇒ χ^2/NDP= 400/34; problems with the flavor disentangling

- Suppressed (fitted) charm distribution requires corresponding enhancement of strangeness due to constraint from W data

Thorne QCD@LHC2018

New input: ATLAS at 7 TeV

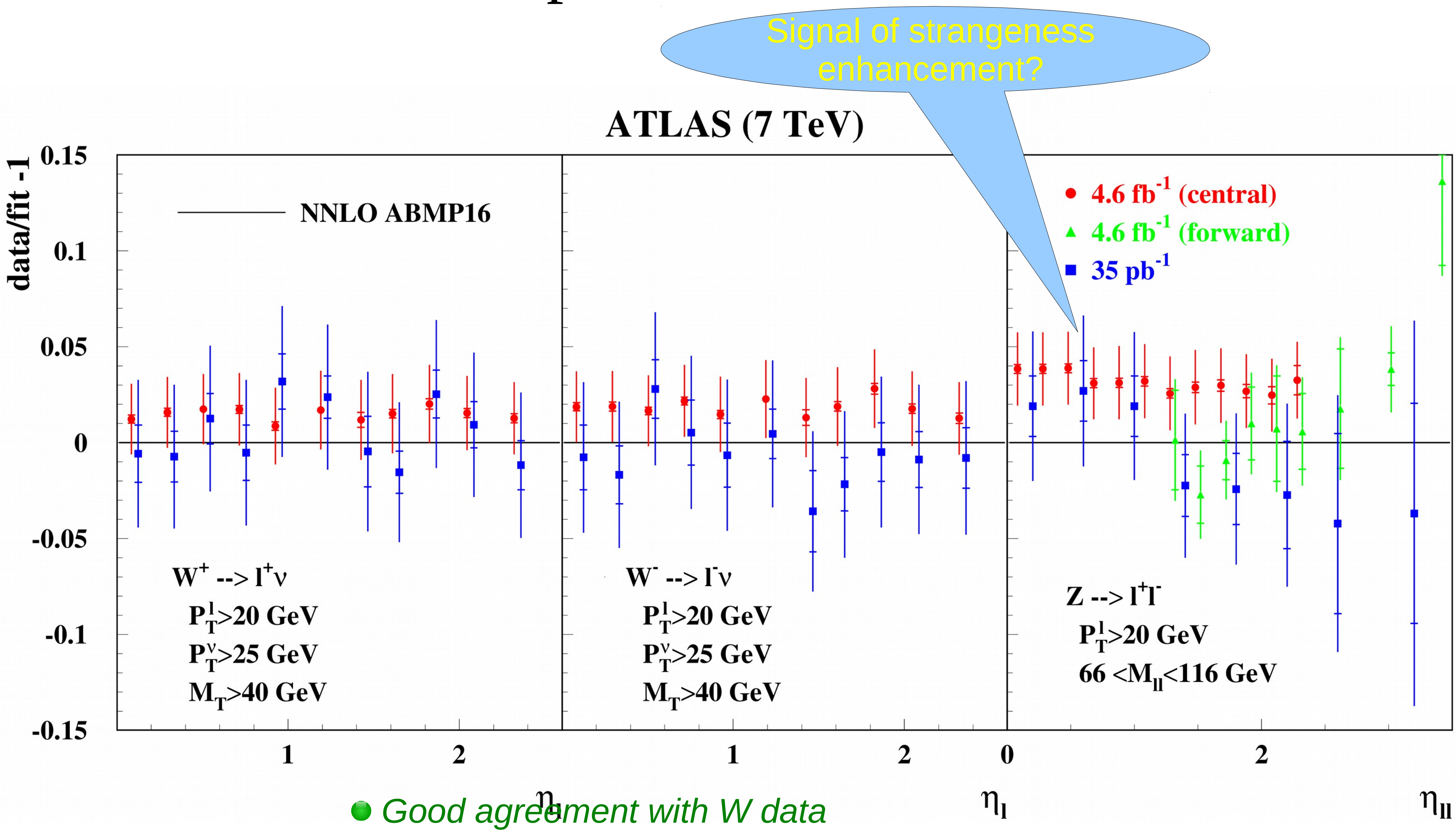

- *Good agreement with W data*
- *Undershooting Z-boson data*
- *Different trends for the central and forward Z-boson data*

CMS data on Z-boson production

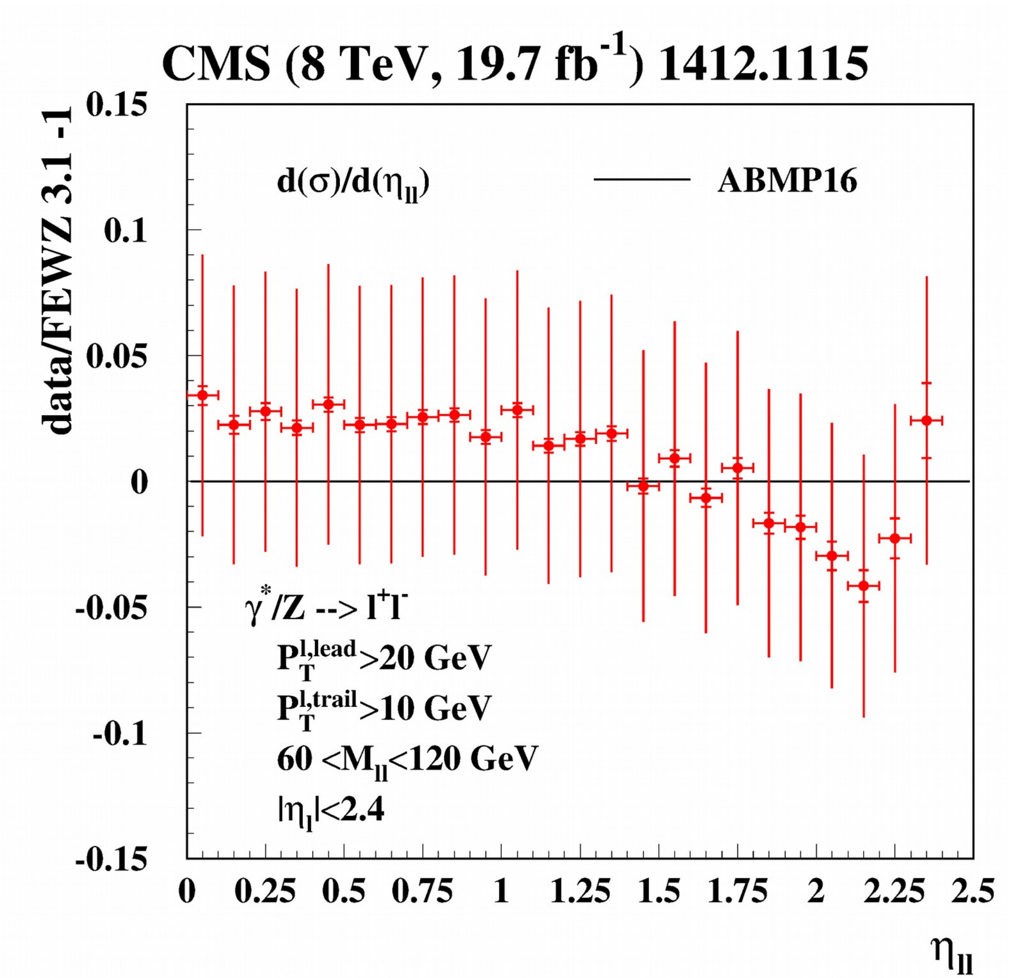

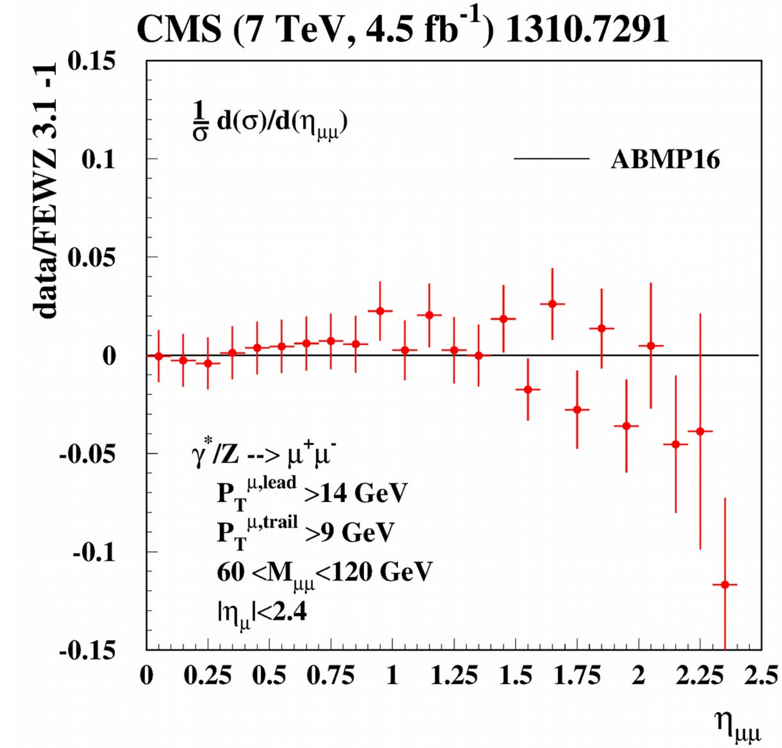

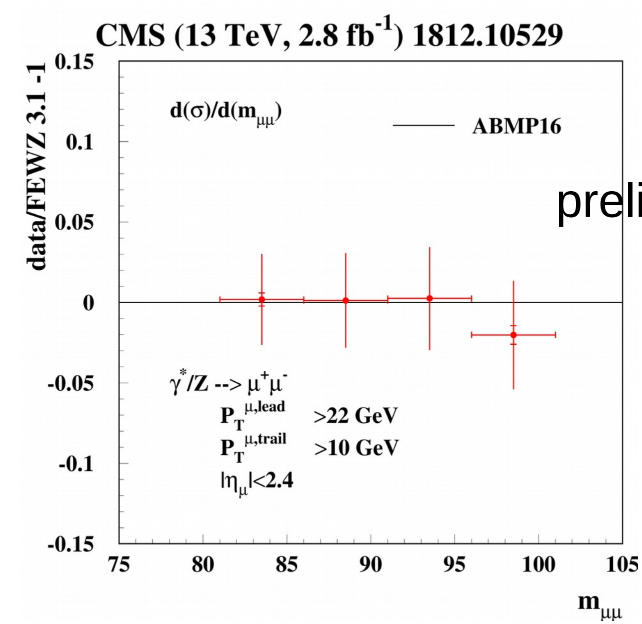

preliminary

The CMS data go somewhat lower than the ATLAS ones and the trend is different at large rapidity; further clarification is necessary

Impact of ATLAS data with flexible PDF shape

	$\kappa_s(\mu^2=20\ GeV^2)$
HERA+ATLAS	0.81(18)
HERA+ATLAS+E866	0.72(8)
ABMP16(incl. NOMAD)	0.66(3)

κ_s is integral strange sea suppression factor:

$$\kappa_s(\mu^2) = \frac{\int_0^1 x[s(x,\mu^2)+\bar{s}(x,\mu^2)]dx}{\int_0^1 x[\bar{u}(x,\mu^2)+\bar{d}(x,\mu^2)]dx},$$

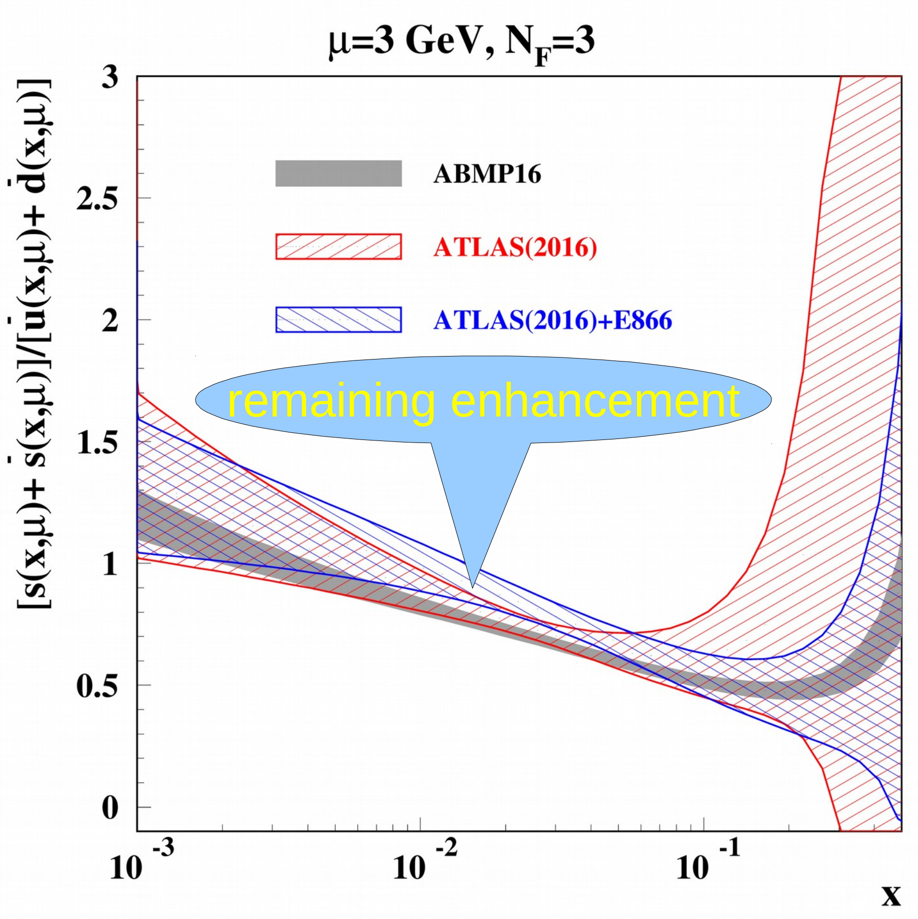

- For the flexible PDF shape the strangeness is in a broad agreement with the one extracted from the dimuon data
- The E866 data are consistent with the ATLAS(2016) set: χ^2/NDP=48/39 and 40/34, respectively.

Summary

- The strange sea suppression observed in the early νN DIS experiments is confirmed by recent precise measurements (NOMAD, CHORUS)

- These data sets can be accommodated into the global PDF fit with a consistent treatment of the fixed-target and collider Drell-Yan data

- The ATLAS analysis based on the combination of Drell-Yan and HERA DIS data demonstrates strange sea enhancement by the price of disagreement with the Fermilab fixed-target Drell-Yan data (E-866, E-906) and overconstrained PDF shape at small x

- A refined comparison with recent CMS measurements is desirable in order to confirm small strange-sea enhancement at x~0.01 driven by the recent ATLAS Drell-Yan data

EXTRAS

CHORUS charm data

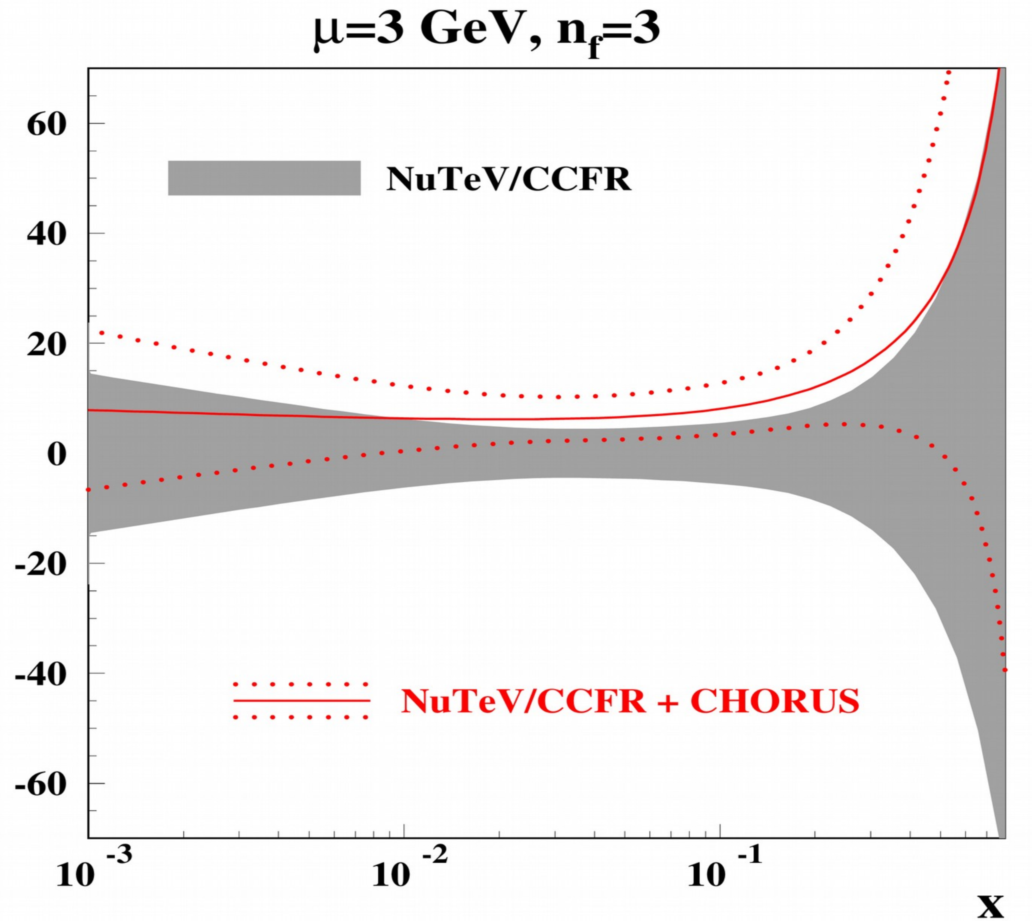

Emulsion data on charm/CC ratio with the charmed hadron vertex measured

CHORUS NJP 13, 093002 (2011)

– full phase space measurements

– no sensitivity to B_μ

– low statistics (2013 events)

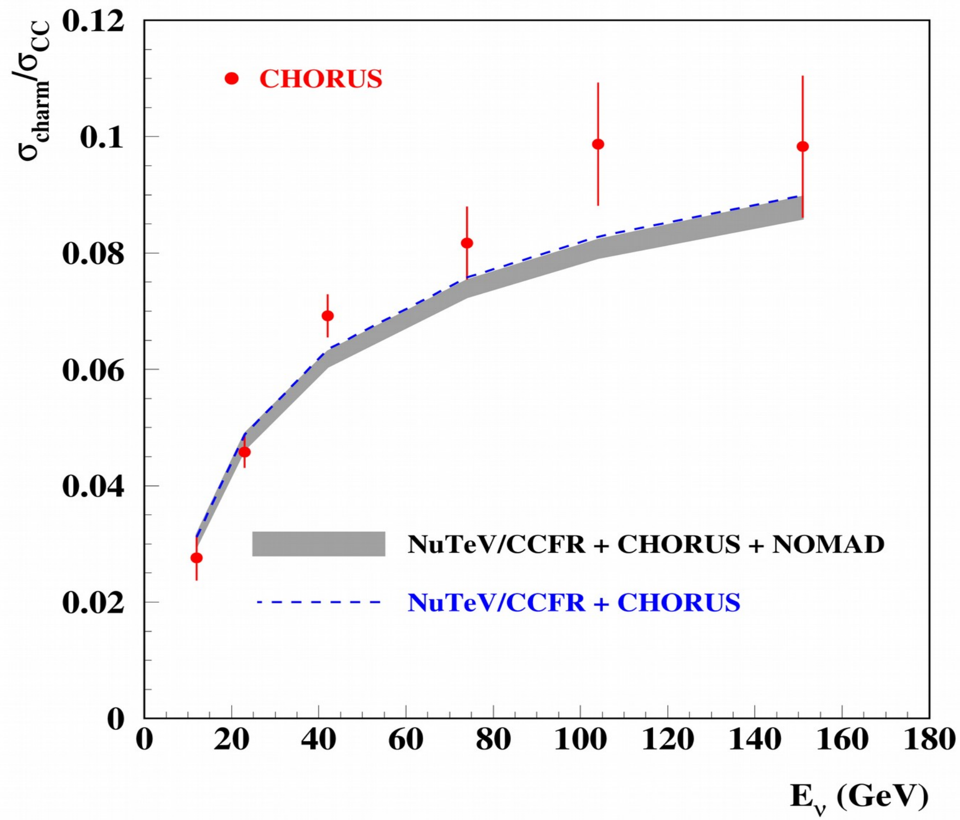

CHORUS data pull strangeness up, however the statistical significance of the effect is poor

sa, Blümlein, Caminada, Lipka, Lohwasser, Moch, Petti, Placakyte hep-ph/1404.6469

CMS W+charm data

CMS Collaboration JHEP 02, 013 (2014)

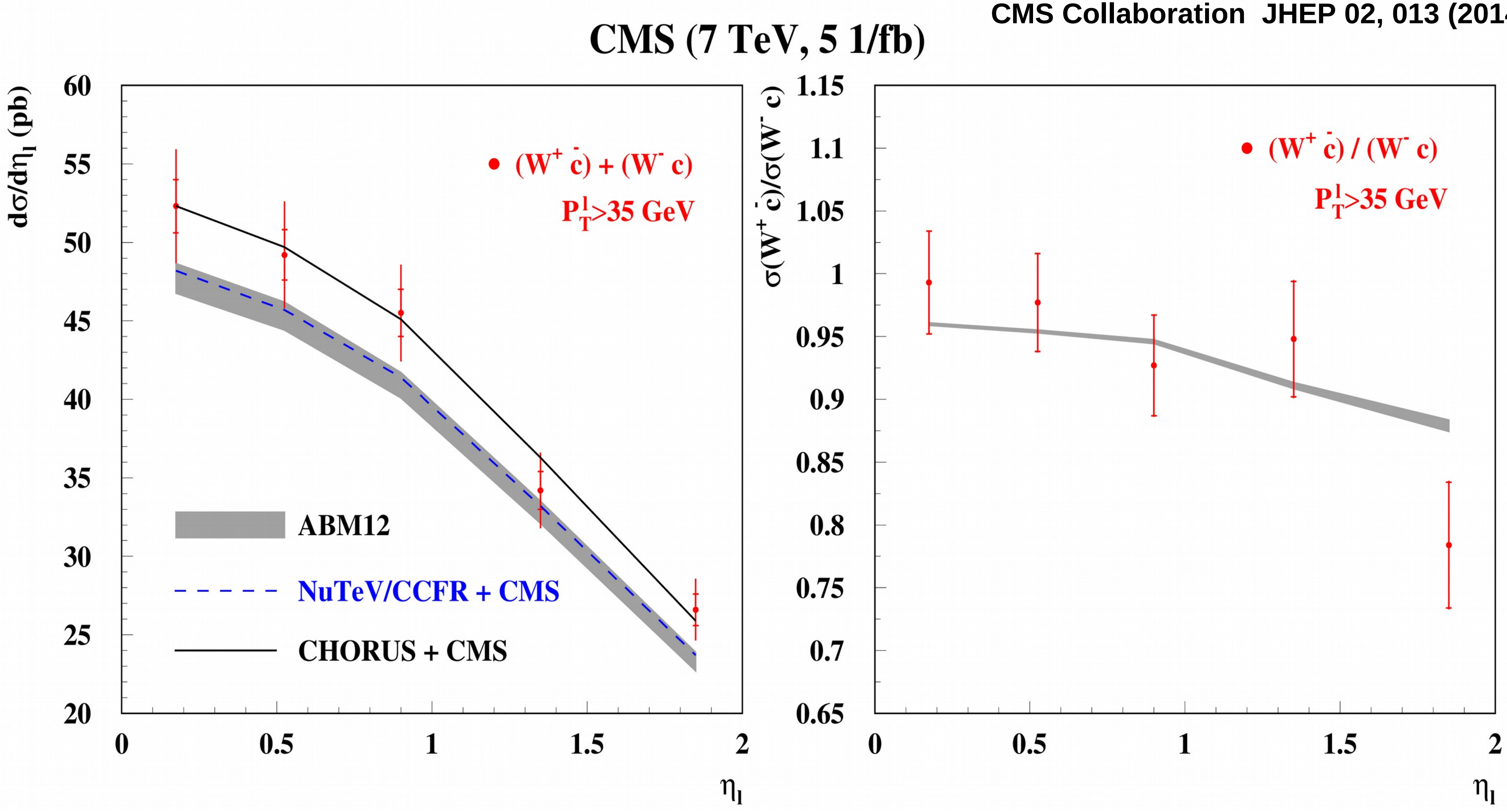

- CMS data go above the NuTeV/CCFR by 1σ; little impact on the strange sea
- The charge asymmetry is in a good agreement with the charge-symmetric strange sea
- Good agreement with the CHORUS data

ATLAS W+charm data

ATLAS arXiv:1402.6263

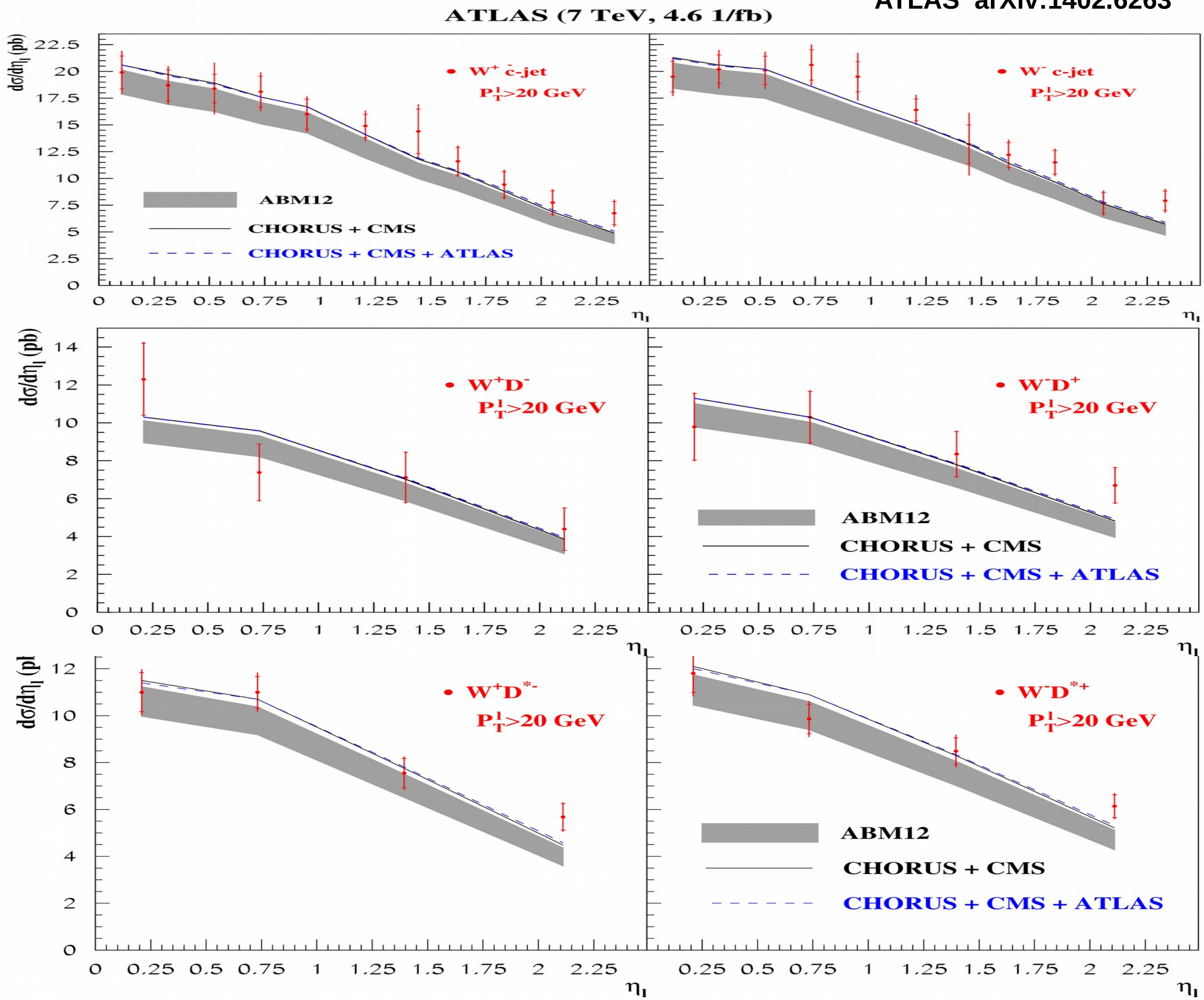

Details of the epWZ and ABMP16 fits

	epWZ16	ABMP16
Data	HERA, ATLAS W&Z	HERA, LHC and Tevatron W&Z, fixed-target DIS and charm production, fixed-target DY, ….
PDF shape	$xu_v(x,\mu_0^2) = A_{u_v} x^{B_{uv}} (1-x)^{C_{uv}} (1+E_{u_v} x^2)$, $xd_v(x,\mu_0^2) = A_{d_v} x^{B_{dv}} (1-x)^{C_{d_v}}$, $x\bar{u}(x,\mu_0^2) = A_{\bar{u}} x^{B_{\bar{u}}} (1-x)^{C_{\bar{u}}}$, $x\bar{d}(x,\mu_0^2) = A_{\bar{d}} x^{B_{\bar{d}}} (1-x)^{C_{\bar{d}}}$, $xg(x,\mu_0^2) = A_g x^{B_g} (1-x)^{C_g} - A'_g x^{B'_g} (1-x)^{C'_g}$, $x\bar{s}(x,\mu_0^2) = A_{\bar{s}} x^{B_{\bar{s}}} (1-x)^{C_{\bar{s}}}$, 15 free parameters	$xq_v(x,\mu_0^2) = \frac{2\delta_{qu}+\delta_{qd}}{N_q^v} (1-x)^{b_{qv}} x^{a_{qv} P_{qv}(x)}$, $xq_s(x,\mu_0^2) = A_{qs} (1-x)^{b_{qs}} x^{a_{qs} P_{qs}(x)}$, $xg(x,\mu_0^2) = A_g (1-x)^{b_g} x^{a_g P_g(x)}$, $P_p(x) = (1+\gamma_{-1,p} \ln x)\left(1+\gamma_{1,p} x + \gamma_{2,p} x^2 + \gamma_{3,p} x^3\right)$, 25 free parameters

ABMP16 PDFs are selected more flexible in order to accommodate more data as compared to the EpWZ16 fit, which was evolved form the HERA data analysis

NNLO tools benchmarking

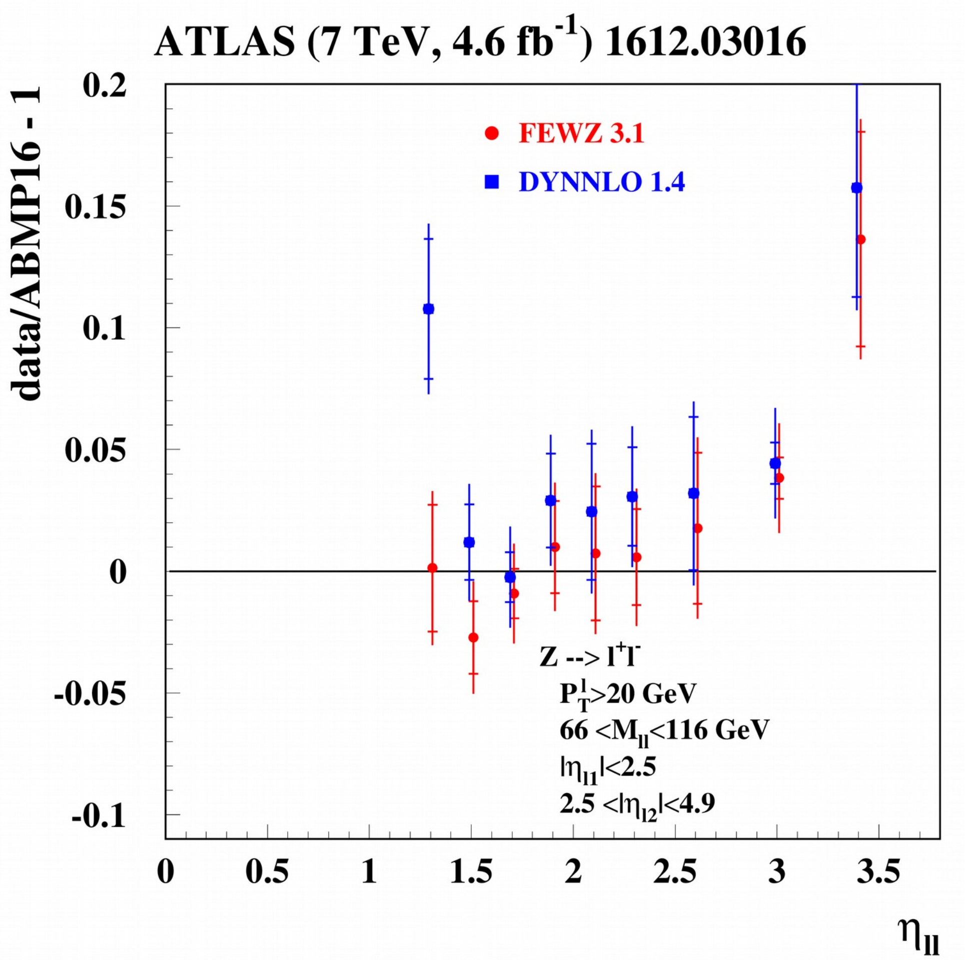

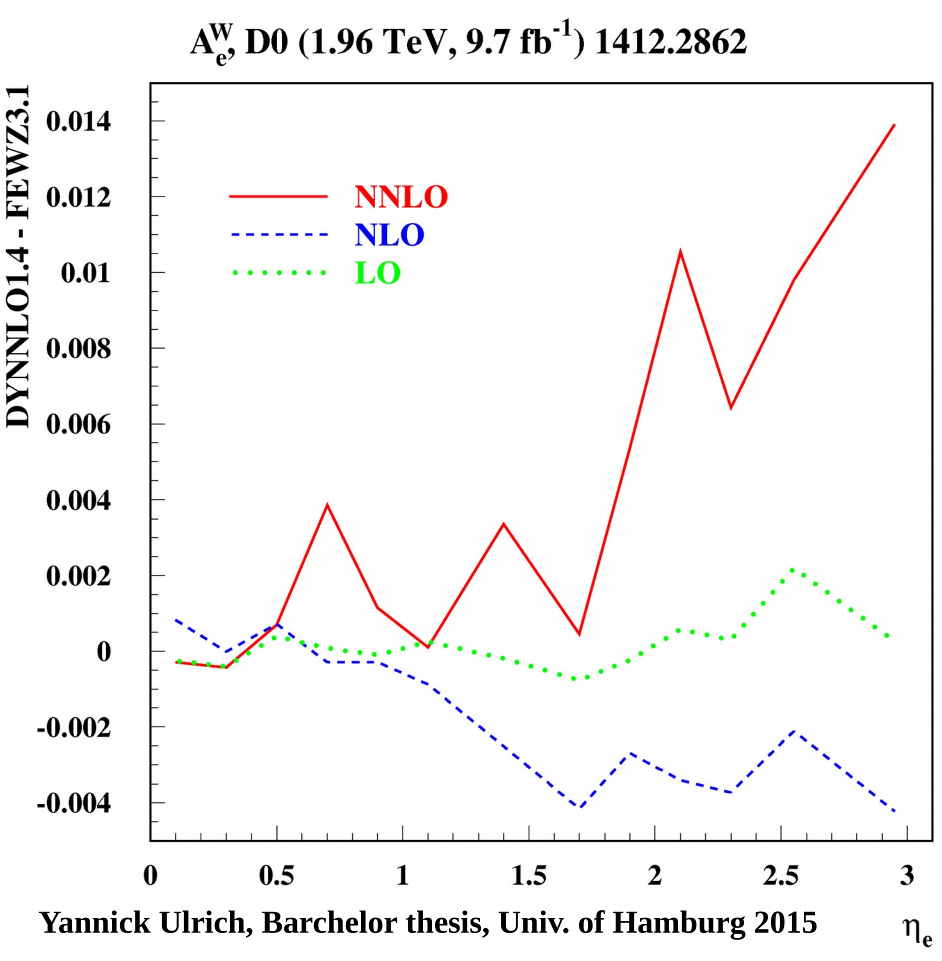

DYNNLO-FEWZ difference not fully understood; further benchmarking is needed

LHC data on Z-boson production